Geological Survey of Japan Cruise Report No. 23, p. 187-200, 1994

X. CHEMICAL AND TEXTURAL VARIATIONS WITHIN MANGANESE NODULES OF THE PENRHYN BASIN, SOUTH PACIFIC (GH83-3 AREA)

Kenichi Harada, Kazuya Higashitani*, Jai-Ho Choi*, and Akira Usui*

Introduction

Manganese nodules in the Penrhyn Basin are characterized by a wide range of morphological variety (Usui, Chapter VIII of this volume). Although the nodules are subdivided into twelve morphological types based on shape, size and surface texture ("grain size" of the surface knobs) (Yagi, 1987), they belong in appearance to Type "s" (smooth) of Moritani *et al.* (1977). A preliminary study on nineteen small spherical nodules (Choi, 1986) and a synthetic mineralogical study of this area (Usui and Mita, Chapter IX of this volume) revealed that the major manganese mineral of the growth layers is vernadite but a small amount of buserite is identified by XRD only in the outer layers of some nodules. Their bulk chemical composition indicates hydrogenetic origin and a moderate enrichment of cobalt. A remarkably similar appearance, dark-brown smooth surface of the outer layers, suggests that they have formed under a fairly constant condition prevailed over the area. As the nodules occur well below the CCD, no calcareous nannofossils were observed as impressions (Harada and Nishida, 1976) under SEM. No siliceous fossils such as diatoms and radiolarians were extracted either from the residues of growth layers treated with hydrochloric acid (Harada *et al.*, 1981).

In this study fourteen nodules with spherical shape but different sizes were selected for observations of internal structure and for chemical analysis to examine the growth history and the relationship between chemical composition and internal structures.

Materials and method

The fourteen spherical nodules of different diameters were selected for chemical and microstructural analyses (Table X-1, Fig. X-1). The original position of nodules on the sea floor was examined from attached sediments only on the bottom side. When the sediment is not attached, the smoother surface was assumed to present the top side. The air-dried specimens at room temperature were soaked in gelatin solution under decompression for half a day. After solidification at room temperature, each specimen was vertically cut into halves with a handy scroll saw. For reflection microscopic

* Department of Earth Sciences, Yamagata University. Koshirakawa-cho, Yamagata.

Keywords: manganese nodule, chemical composition, internal structure, morphology, growth history, bottom current, Manihiki Plateau, Hakurei-Maru, Penrhyn Basin

Table X-1 Location data and simple description of the nodules studied.

Sample No.	Location		Water depth	Surface sediment	SBP Unit	Dimension	Dry weight	Shape
	latitude (S)	longitude (W)	m			cm	g	
FG627	13°14.85'	159°29.96	5263	pelagic clay	II?	2.7 x 2.1 x 1.0	9.1	coating
FG638	12°59.09'	159°12.58	5215	pelagic clay	II	3.5 x 3.2 x 3.2	38.8	ellipsoidal
FG641	13°02.22'	159°11.38	5222	pelagic clay	II	2.5 x 1.2 x 1.6	11.2	ellipsoidal
FG657	12°58.63'	158°57.33	5114	zeolitic clay	I	2.2 x 2.1 x 2.2	9.5	spheroidal
FG664-A	12°05.39'	159°08.72	5206	zeolite rich clay	II	1.2 x 1.1 x 1.2	1.3	ellipsoidal
FG664-B	do.	do.	do.	do.	do.	1.5 x 1.1 x 1.1	2.0	ellipsoidal
FG686	13°16.66'	159°11.43	5173	zeolite lich clay	II	6.4 x 5.9 x 5.9	178.2	spheroidal
FG691-S	13°06.49'	159°17.23	5209	pelagic clay	II	2.3 x 2.3 x 2.2	8.8	ellipsoidal
FG691-M	do.	do.	do.	do.	do.	3.0 x 2.9 x 3.1	28.9	spheroidal
FG691-L	do.	do.	do.	do.	do.	4.1 x 3.5 x 3.9	41.1	ellipsoidal
FG706-S	13°08.60'	159°18.67	5224	zeolite-rich clay	II	1.9 x 1.7 x 1.7	5.8	discoidal
FG706-M	do.	do.	do.	do.	do.	3.6 x 3.1 x 2.7	21.9	ellipsoidal
FG706-L	do.	do.	do.	do.	do.	4.6 x 4.6 x 4.1	70.8	discoidal
D535-1	13°00.14'	159°17.59	5222	-	II	2.5 x 2.5 x 2.4	14.8	spheroidal

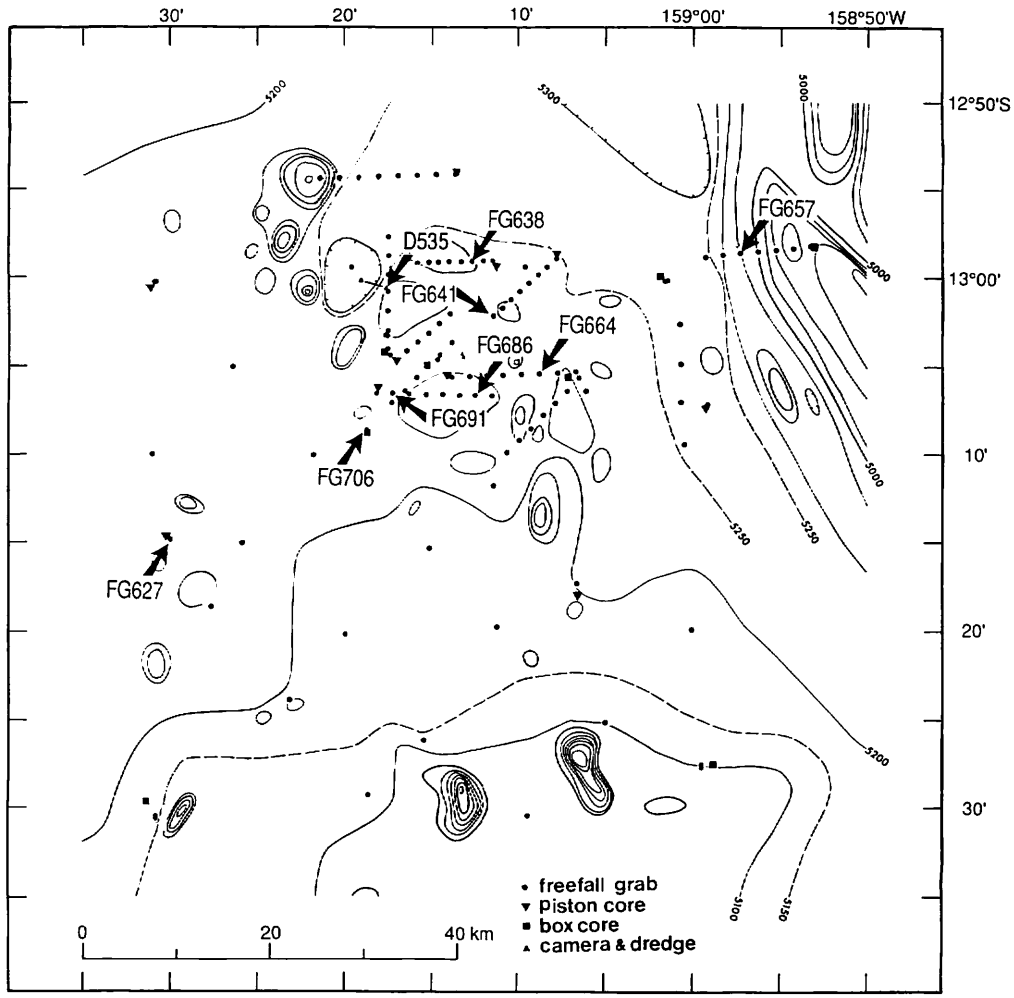

Fig. X-1 Location map of the studied nodules. See Usui (Chapter III) for the acoustic stratigraphy.

observation, one half was polished by the method described by Sorem and Fewkes (1980). The other half was rinsed with warm water to dissolve the disseminated gelatin within nodules. Layer-by-layer subsamples were carefully scraped both from the upper and lower hemispheres under binocular microscope. Chemical analysis was done for Fe, Mn, Cu, Ni and Co by an atomic-absorption spectrometer (Hitachi 209) according to the analytical guidelines of the Geological Survey of Japan (Terashima, 1978). The accuracy of analysis was approximately within $\pm 3\%$.

Description and discussion

Internal Structure

All the nodules studied have a small nucleus of various material such as, altered volcanic rocks, zeolitic stones, and a fragment of older nodules (Table 2) around

Table X-2 Thickness of each growth unit of the nodules. Components of nucleus are based on field observation.

Sample No.	FG627	FG638	FG641	FG657	FG664A	FG664B	FG686	FG691S	FG691M	FG691L	FG706S	FG706M	FG706L	D535-1
Mn oxide layers														
thickness (mm)														
Layer A	0.60	0.30	0.30	0.25	0.45	0.40	0.60	0.20	0.60	0.75	0.60	0.75	0.60	0.45
Layer B	0.30	-	0.30	0.60	0.60	0.60	0.75	0.45	0.30	0.45	0.60	0.30	0.30	0.45
Layer C	nd	6.30	4.60	2.10	0.90	0.90	16.00	3.30	4.80	7.50	4.50	4.20	4.80	3.90
Layer D	-	1.20	1.80	3.00	-	-	2.00	1.50	1.80	3.50	1.80	2.60	3.00	3.30
Layer E	-	-	-	-	-	-	2.20	-	-	-	-	-	1.50	-
Layer F	-	-	-	-	-	-	13.30	-	-	-	-	-	3.00	-
total	0.90	7.80	7.00	5.95	1.95	1.90	34.85	5.45	7.50	12.20	7.50	7.85	13.20	8.10
Nucleus														
diameter (mm)	6.50	7.40	6.50	6.50	3.40	4.00	2.50	5.00	9.00	10.10	4.00	3.50	7.50	2.00
components	nodule fragment	disseminated tuff	phosphorite?	phosphorite?	zeolitic claystone	zeolitic claystone	tuff	nodule fragment	nodule fragment	tuff?	nodule fragment	tuff?	tuff?	tuff?

which the concentric growth layers develop. The larger nodules have the more identifiable layers of growth units. No significant break (unconformity) in the growth units was observed under the microscope. Figure X-2 demonstrates a schematic nodule stratigraphy according to the textural criteria of this study.

The outermost layer of approximately 1 mm thickness encrusts the entire nodules and is easily scraped from the surface except for the upper part of Samples FG664A and FG664B. The layer consists of two units with different structures. The outer part, Layer A, shows a columnar structure and contains small amounts of phillipsite. The inner part with laminated structure, Layer B, has a metallic luster and shows high reflectivity under the microscope. Although anisotropy was not clearly seen, probably due to the submicroscopic size of the crystals, the laminated part possibly contain the buserite phase of Usui (1979). Layers A and B develop in all nodules, but Sample FG638 lacks Layer B. Sample FG638 contains an intercalary layer beneath Layer A in the lower hemisphere, which is subdivided into the inner Layer S1 (ca. 3 mm thick) and the outer Layer S2 (ca. 1 mm thick).

Beneath Layers A and B, the thicker Layer C is defined. This layer is characterized by a fan-shaped columnar structure in the inner part and a normal columnar one in the outer part. As the fan-shaped columnar structure is porous, coarser sedimentary particles such as phillipsite crystals fill the vacant spaces between the columns. The fill-in sediments are less developed in the outer part with dense columns. Layer C is common to all the nodules except in the upper hemisphere of Sample FG627. The inner part of Layer C of Sample FG641 is subdivided into Layers C and C'. Layer C of Samples FG664A and FG664B was not able to be separated, so the sample were excluded from the chemical analysis.

Layer D develops just over the nucleus of moderate-size nodules (FG657-FG706M in Fig. X-2). The layer mainly consists of the columnar structure, but partly contains the fan-shape structure. Layers C and D are bounded by thin clayey laminae. In the bottom hemisphere of Sample FG638, an intercalary layer named as Layer EX (ca. 3 mm thick) was additionally analyzed.

In the large nodules, Samples FG686 and FG706L, the additional two layers develop below Layer D around the nucleus: a thin outer Layer E with a laminated structure and a thicker inner Layer F with the fan-shaped columnar structure. In the lower part of Layer F, a colloform structure with high reflectivity were observed in part.

In general, the schematic microstructural stratigraphy of nodules (Figure X-2), described by microscopic observation, well demonstrates several stages of nodule growth. The larger nodules started to grow possibly at the Paleogene time (Nishimura and Saito, Chapter IV; Usui and Mita, Chapter IX of this volume) and contain the oldest growth units (Layers E and F). The smaller nodules started to grow at much younger ages when the nuclei were supplied on the basin floor.

Chemical composition

The contents of Fe, Mn, Cu, Ni and Co in each growth unit are listed in Table 3. The compositional variations of each growth unit within each nodule are shown in Figures X-3, X-4 and X-5. It is noted that the depth profiles of metal concentrations

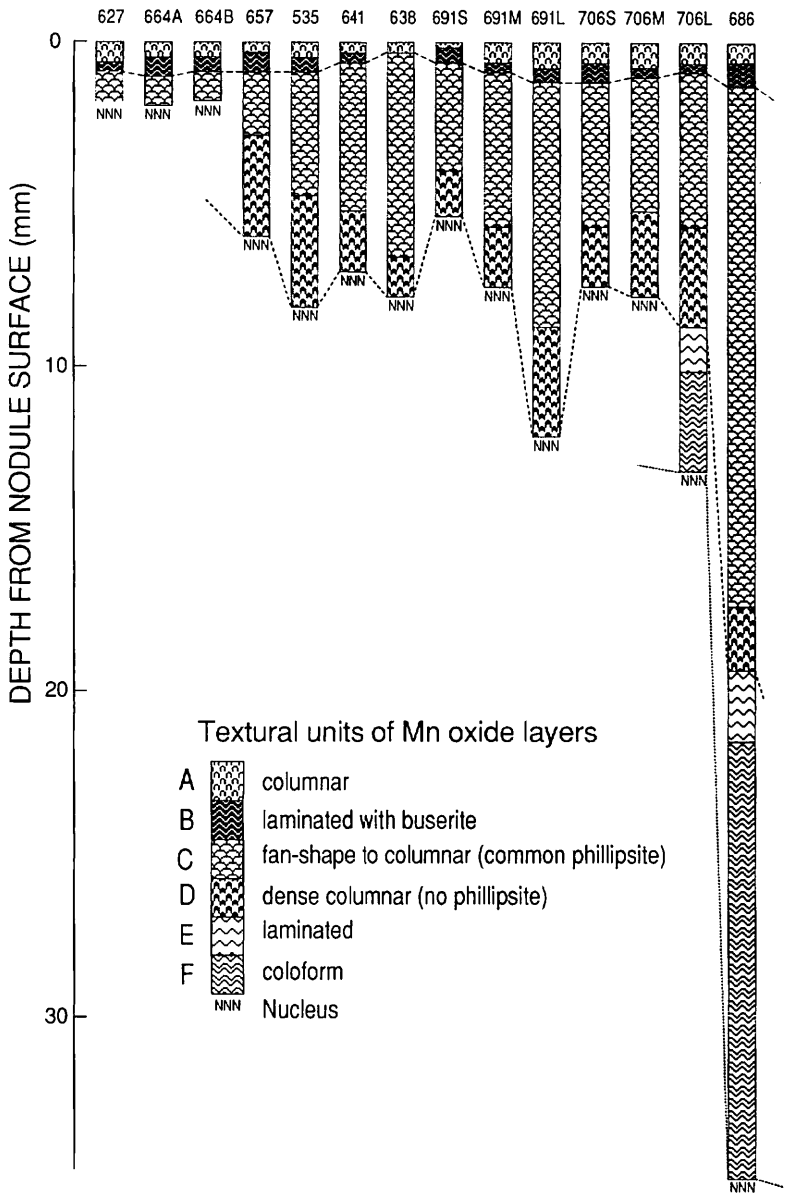

Fig. X-2 Schematic stratigraphy of the nodules based on microstructures under the microscope. Note fairly constant thickness of each layer and well correlated boundaries (dotted lines) between the nodules of different sites.

Table X-3 Chemical composition of the growth layers of manganese nodules.

No.	part	unit	Fe	Mn	Cu	Ni	Co	Mn/Fe
FG535	upper	A	20.3	12.3	0.108	0.217	0.525	0.61
	upper	B	19.4	15.3	0.277	0.575	0.510	0.79
	upper	C	14.6	15.5	0.156	0.288	0.498	1.06
	upper	D	12.4	14.6	0.133	0.355	0.410	1.18
	lower	D	12.4	14.9	0.137	0.359	0.430	1.20
	lower	C	14.8	15.4	0.149	0.250	0.480	1.04
	lower	B	18.5	15.3	0.309	0.584	0.467	0.83
	lower	A	18.0	15.0	0.146	0.256	0.541	0.83
	Average		16.3	14.8	0.177	0.361	0.483	0.91
FG627	upper	A	16.1	13.9	0.119	0.197	0.474	0.86
	upper	B	14.0	17.0	0.401	0.612	0.409	1.21
	upper	C	12.7	16.0	0.301	0.503	0.445	1.26
	lower	B	16.8	14.1	0.195	0.605	0.504	0.84
	lower	A	21.1	10.6	0.210	0.480	0.402	0.50
	Average		16.1	14.3	0.245	0.479	0.447	0.89
FG638	upper	A	17.4	13.4	0.229	0.396	0.455	0.77
	upper	C	13.4	16.6	0.158	0.278	0.561	1.24
	upper	D	10.2	17.8	0.198	0.643	0.435	1.75
	lower	D	10.2	18.6	0.179	0.648	0.506	1.82
	lower	E	12.1	15.9	0.111	0.341	0.446	1.31
	lower	C	15.1	16.8	0.115	0.309	0.524	1.11
	lower	S1	20.1	12.6	0.086	0.153	0.561	0.63
	lower	S2	20.7	12.9	0.127	0.304	0.475	0.62
	lower	A	20.5	11.9	0.136	0.309	0.421	0.58
	Average		15.5	15.2	0.149	0.376	0.487	0.98
FG641	upper	A	18.7	12.8	0.221	0.391	0.462	0.68
	upper	B	16.9	16.8	0.321	0.636	0.482	0.99
	upper	C	14.3	16.7	0.163	0.327	0.531	1.17
	upper	C'	13.3	14.5	0.122	0.278	0.486	1.09
	upper	D	12.5	15.5	0.124	0.334	0.422	1.24
	lower	D	12.2	14.4	0.124	0.315	0.369	1.18
	lower	C'	11.9	13.7	0.115	0.262	0.377	1.15
	lower	C	13.7	16.1	0.172	0.334	0.454	1.18
	lower	B	14.1	17.9	0.326	0.771	0.486	1.27
	lower	A	20.0	13.0	0.185	0.345	0.493	0.65
	Average		14.8	15.1	0.187	0.399	0.456	1.03

No.	part	unit	Fe	Mn	Cu	Ni	Co	Mn/Fe
FG657	upper	A	18.2	15.6	0.256	0.530	0.563	0.86
	upper	B	14.3	18.8	0.404	0.737	0.479	1.31
	upper	C	13.6	17.8	0.235	0.456	0.473	1.31
	upper	D	11.5	16.6	0.209	0.506	0.351	1.44
	lower	D	12.1	16.6	0.222	0.524	0.370	1.37
	lower	C	13.5	17.9	0.253	0.512	0.439	1.33
	lower	B	14.6	18.4	0.356	0.627	0.487	1.26
	lower	A	17.5	15.6	0.287	0.528	0.454	0.89
	Average		14.4	17.2	0.278	0.553	0.452	1.19
FG664A	lower	B	14.4	18.0	0.377	0.648	0.359	1.25
	lower	A	17.3	15.7	0.195	0.376	0.445	0.91
	Average		15.9	16.9	0.286	0.512	0.402	1.06
FG664B	lower	B	13.3	13.4	0.260	0.451	0.271	1.01
	lower	A	20.7	12.9	0.152	0.264	0.417	0.62
	Average		17.0	13.2	0.206	0.358	0.344	0.77
FG686	upper	A	17.2	14.3	0.116	0.246	0.609	0.83
	upper	B	18.5	15.1	0.203	0.550	0.533	0.82
	upper	C	12.0	16.2	0.151	0.392	0.547	1.35
	upper	D	9.6	16.9	0.227	0.522	0.349	1.76
	upper	E	9.4	17.7	0.205	0.615	0.290	1.88
	upper	F	15.5	11.8	0.132	0.245	0.111	0.76
	lower	F	14.5	12.0	0.134	0.283	0.083	0.83
	lower	E	10.7	16.0	0.157	0.418	0.291	1.50
	lower	D	10.0	15.3	0.188	0.458	0.342	1.53
	lower	C	11.3	16.5	0.139	0.370	0.562	1.46
	lower	B	18.0	21.2	0.224	0.509	0.464	1.18
	lower	A	16.6	13.3	0.082	0.193	0.578	0.80
	Average		13.6	15.5	0.163	0.400	0.397	1.14

Table X-3 (continued)

No.	part	unit	Fe	Mn	Cu	Ni	Co	Mn/Fe
FG691S	upper	A	16.5	15.7	0.136	0.312	0.477	0.95
	upper	B	19.3	14.3	0.284	0.535	0.424	0.74
	upper	C	14.4	17.0	0.165	0.344	0.541	1.18
	upper	D	12.3	15.8	0.137	0.359	0.426	1.28
	lower	D	12.3	15.9	0.144	0.373	0.419	1.29
	lower	C	14.2	16.3	0.151	0.344	0.520	1.15
	lower	B	17.5	16.4	0.268	0.653	0.510	0.94
	lower	A	18.9	13.6	0.110	0.219	0.486	0.72
	Average		15.7	15.6	0.174	0.392	0.475	1.00
FG691M	upper	A	20.5	11.6	0.128	0.217	0.492	0.57
	upper	B	18.7	15.5	0.240	0.532	0.585	0.83
	upper	C	13.7	16.3	0.107	0.276	0.560	1.19
	upper	D	12.1	17.5	0.130	0.453	0.477	1.45
	lower	D	12.3	17.4	0.128	0.437	0.462	1.41
	lower	C	13.7	16.8	0.127	0.316	0.554	1.23
	lower	B	17.8	16.3	0.228	0.498	0.564	0.92
	lower	A	15.6	14.8	0.106	0.211	0.553	0.95
	Average		15.6	15.8	0.149	0.368	0.531	1.01
FG691L	upper	A	16.6	14.9	0.152	0.317	0.579	0.90
	upper	B	18.5	15.7	0.252	0.544	0.607	0.85
	upper	C	14.1	16.3	0.122	0.298	0.565	1.16
	upper	D	12.7	16.5	0.193	0.655	0.233	1.30
	lower	D	12.6	17.7	0.189	0.627	0.345	1.40
	lower	C	14.5	16.0	0.134	0.324	0.521	1.10
	lower	B	18.7	14.6	0.186	0.470	0.525	0.78
	lower	A	18.8	14.7	0.058	0.153	0.570	0.78
	Average		15.8	15.8	0.161	0.424	0.493	1.00

No.	part	unit	Fe	Mn	Cu	Ni	Co	Mn/Fe
FG706S	upper	A	18.6	13.9	0.182	0.331	0.442	0.75
	upper	B	15.0	18.1	0.379	0.644	0.382	1.21
	upper	C	13.4	16.7	0.210	0.368	0.392	1.25
	upper	D	11.2	17.7	0.214	0.437	0.415	1.58
	lower	D	11.9	16.3	0.147	0.347	0.348	1.37
	lower	C	14.1	16.7	0.204	0.374	0.434	1.18
	lower	B	17.8	15.9	0.281	0.464	0.422	0.89
	lower	A	20.7	12.8	0.182	0.312	0.406	0.62
	Average		15.3	16.0	0.225	0.410	0.405	1.04
FG706M	upper	A	19.1	13.8	0.073	0.152	0.478	0.72
	upper	B	19.5	13.9	0.280	0.450	0.376	0.71
	upper	C	14.2	17.0	0.133	0.289	0.479	1.20
	upper	D	11.4	16.2	0.130	0.340	0.413	1.42
	lower	D	10.0	16.2	0.142	0.402	0.266	1.62
	lower	C	14.2	15.3	0.148	0.292	0.393	1.08
	lower	B	16.5	16.3	0.222	0.460	0.486	0.99
	lower	A	16.4	15.1	0.159	0.255	0.484	0.92
	Average		15.2	15.5	0.161	0.330	0.422	1.02
FG706L	upper	A	17.6	13.8	0.089	0.171	0.461	0.78
	upper	B	16.0	16.3	0.203	0.389	0.540	1.02
	upper	C	14.8	15.8	0.148	0.301	0.490	1.07
	upper	D	12.1	17.1	0.180	0.514	0.439	1.41
	upper	E	13.0	17.6	0.260	0.698	0.212	1.35
	upper	F	14.3	16.2	0.210	0.506	0.163	1.13
	lower	F	14.8	15.0	0.235	0.555	0.115	1.01
	lower	E	12.7	16.2	0.260	0.697	0.177	1.28
	lower	D	13.0	14.3	0.138	0.269	0.399	1.10
	lower	C	14.8	15.7	0.132	0.219	0.457	1.06
	lower	B	16.4	19.4	0.289	0.397	0.398	1.18
	lower	A	16.2	14.3	0.188	0.254	0.442	0.88
	Average		14.6	16.0	0.194	0.414	0.358	1.09

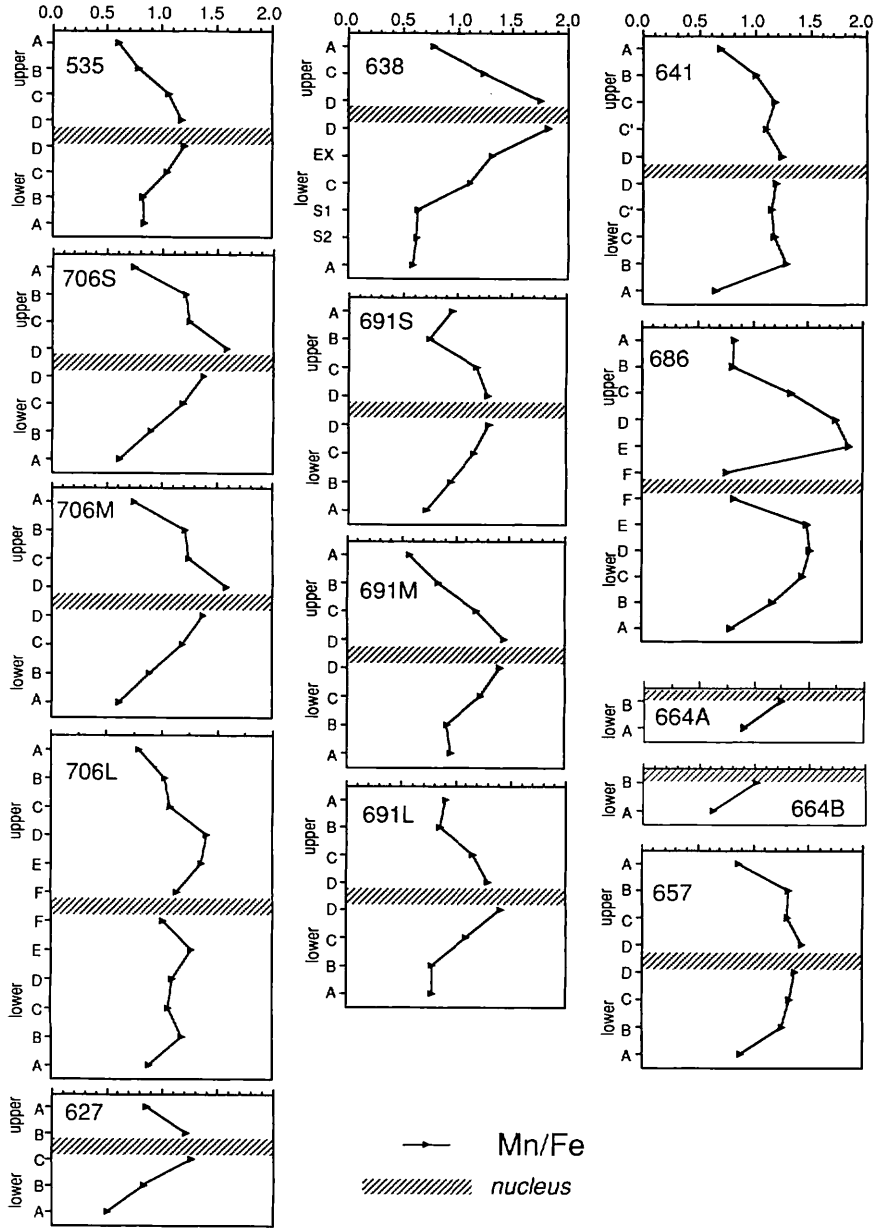

Fig. X-3 Internal variations of the Mn/Fe ratio of the growth units from the nuclei to the surface.

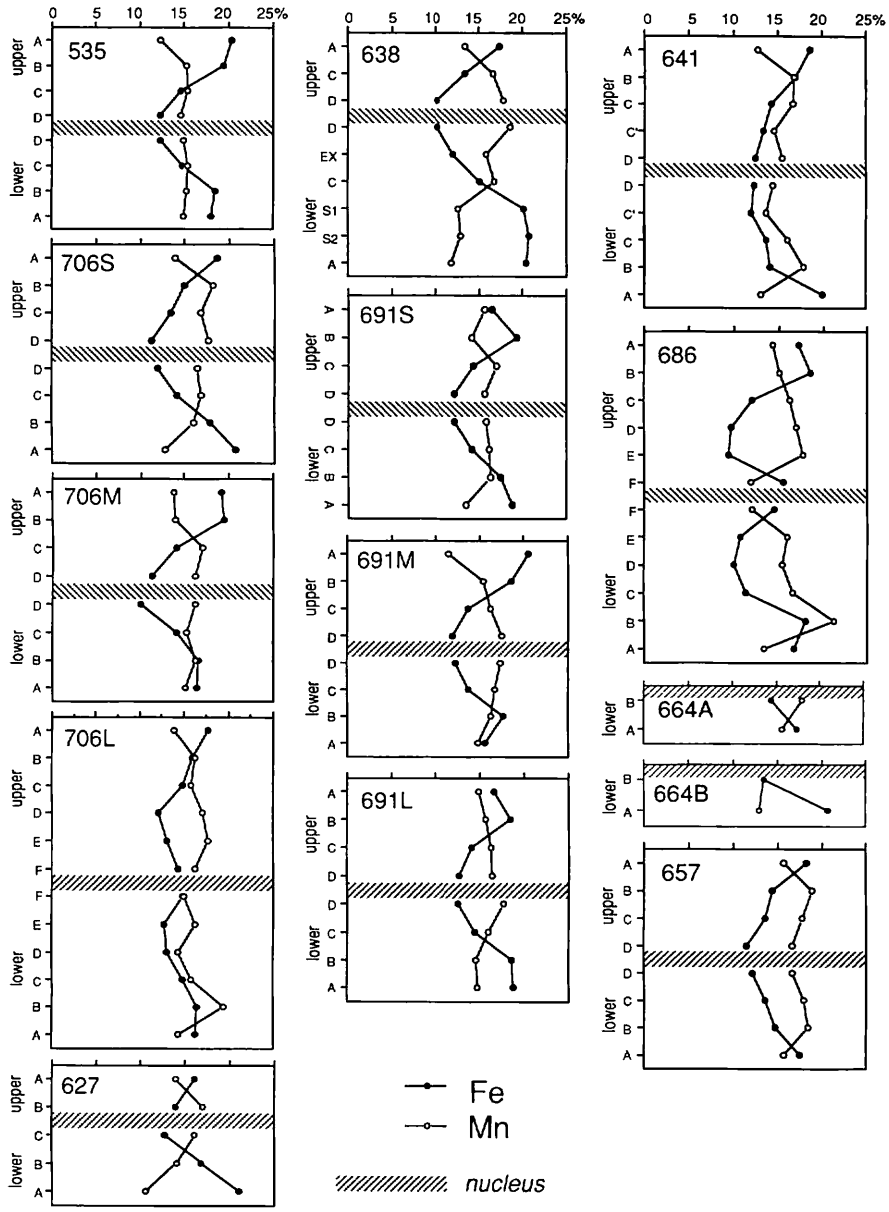

Fig. X-4 Internal variations of concentrations of Mn and Fe of the growth units from the nuclei to the surface.

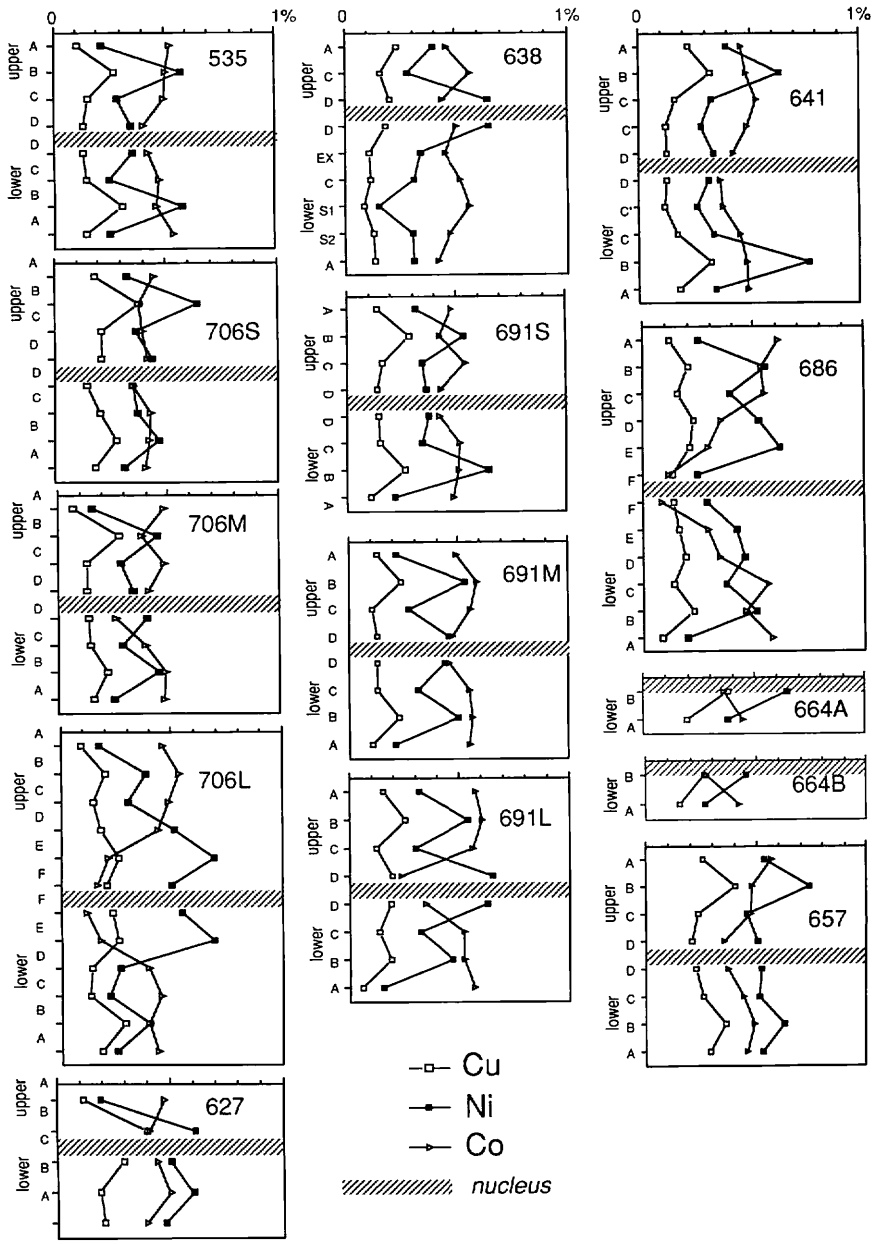

Fig. X-5 Internal variations of concentrations of Cu, Ni and Co of the growth units from the nuclei to the surface.

in the upper and the lower hemispheres show symmetrical patterns. This symmetry in chemical composition, as well as the concentric growth units around the nucleus, indicates that the nodules have accreted over the entire surfaces. As the general chemical characteristics suggest a slow and continuous hydrogenetic growth, the nodules should have occasionally turned over so that their surface was exposed evenly to the sea water during their growth. Since, however, biological activity is low in this basin as evidenced by the soft-X ray radiographs of the surface sediment columns (Nishimura and Saito, Chapter IV of this volume), the moving force of the nodules could not be attributed to the biological activity. Hence, the most probable mechanism for turnover is a prevailing bottom current which swept the sea floor. This might also explain the occurrence of some polynucleated nodules which formed by contact of more than two small nodules during the growth.

Fe content tends to increase outwards (Figs. X-4 and X-6), while Mn slightly decreases outwards. The Cu and Ni concentrations are significantly higher at Layer B (Figs. X-5 and X-6) which are accommodated by buserite (Usui and Mita, Chapter IX of this volume). The nodules of this area may have encountered early diagenetic process of the surface sediments promoted by higher productivity in the water column during the formation of Layer B.

The most prominent depth dependency is the monoclinal increase of Co concentration (or Co/Mn ratio) towards the nodule surface (Fig. X-6). The ratio of average concentrations of Co of Layers A to F is more than 3, and maximum ratio is 7 in FG686. Halbach *et al.* (1982) first pointed out that the Co in ferromanganese crusts decreases with water depth in the range of 1000 to 4000 meters in the Central Pacific seamount areas. They interpreted the depth dependency in relation to the presence of an oxygen minimum zone around the equator. Since there is neither sedimentary nor tectonic evidence of uplifting in the Penrhyn Basin area which may have affected the nodule forming condition, the effect of an oxygen minimum zone should be ruled out. In addition, we find no significant change in mineral composition within nodules.

On the other hand, Manheim (1986) assumes that as the Co flux in the sea water is fairly constant (Halbach *et al.*, 1983), Co concentration in hydrogenetic nodules or crusts can be a function of their growth rate. Assuming a constant Co flux to the nodules of this area, the outward increase of Co content may be attributed to a decrease of the growth rate. The tendency is recognized commonly in the nodules from other areas (Harada and Nishida, 1976; Harada *et al.*, 1985). The measured slow ^{10}Be growth rate in the surface 5 mm layer of one nodule from the area (Inoue, unpublished; also see Usui and Mita, Chapter IX of this volume), 1.07 mm/m.y., agrees well with this interpretation.

The larger nodules have two additional growth bands beneath Layer D. Although their chemical composition suggests a hydrogenetic origin, the compositional difference from those in Layers A- D, may be explained by a change of chemical composition in the deep-sea water (AABW) flowing on the seabed. Further radiochemical dating is, however, needed to corroborate this idea.

In conclusion, this study positively supports an idea that fine-scale variations in chemical composition and microstructure within nodules can reflect the past sedimentary and physico-chemical conditions of the sea floor.

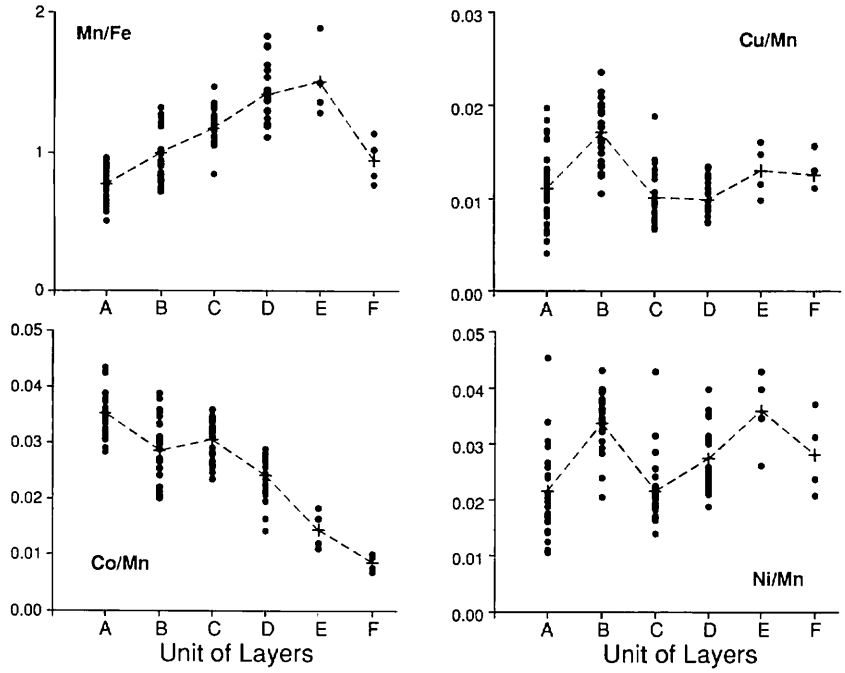

Fig. X-6 Summary of the internal variation in chemical composition. All the upper and lower parts are plotted together except for S1, S2, and EX. Dotted lines combine the averaged values for each units.

References

Choi, J.-H. (1986) *Formation mechanism of the manganese nodules in the Penrhyn Basin, South Pacific.* Master's thesis, Dept. Earth Sci., Yamagata Univ., 76 pp. Unpublished.

Halbach, P., Manheim, F. T. and Otten, P. (1982) Co-rich ferromanganese deposits in the marginal seamount regions of the Central Pacific Basin: Results of Midpac '81. *Ertzmetal*, vol. 35, p. 447-453.

————, Segl, M. and Mangini, A. (1983) Co-fluxes and growth rates in ferromanganese deposits from central Pacific seamount areas. *Nature*, vol. 304, p. 716-719.

Harada, K. and Nishida, S. (1976) Biostratigraphy of some Pacific manganese nodules. *Nature*, vol. 260, p. 770-771.

————, Fukui, N. and Nishida, S. (1981) New observation methods for acid-insoluble residue from marine manganese nodules. *Jour. Geol. Soc. Japan*, vol. 87, p. 87-90.

————, Nishida, S. and Usui, A. (1985) Geologic significance of manganese nodules from seamounts and ridges in the North Philippine Sea. *J. Geographical Soc. Japan* (Chigaku-Zassi), vol. 94, p. 170-180.

Manheim, F. T. (1986) Marine cobalt resources. *Science*, vol. 232, p. 600-608.

Moritani, T., Maruyama, S., Matsumoto, K., Ogitsu, T. and Moriwaki, H. (1977) Description, classification, and distribution of manganese nodules. *Geol. Surv. Japan Cruise Rept.*, no. 8, p. 136-158.

Sorem, R. K. and Fewkes, R. H. (1979) *Manganese Nodules*. Plenum Press, New York, 723 pp.

Terashima, S. (1978) Atomic absorption analysis of Mn, Fe, Cu, Ni, Co, Pb, Zn, Si, Al, Ca, Mg, Na, K, Ti, and Sr in manganese nodules. *Bull. Geol. Surv. Japan*, vol. 29, p. 401-411.

Usui, A. (1979) Nickel and copper accumulation as essential elements in 10-Å manganite of deep-sea manganese nodules. *Nature*, vol. 279, p. 411-413.

Yagi, R. (1987) *Morphological classification of manganese nodules in the Penrhyn Basin, South Pacific.* Graduation thesis, Dept. Earth Sciences, Yamagata Univ., 46pp. Unpublished.